MethodsX 12 (2024) 102604

Contents lists available at ScienceDirect

MethodsX

journal homepage: www.elsevier.com/locate/methodsx

Assessing thermoelectric membrane distillation performance: An experimental design approach

Olawale Makanjuola[a,b], Raed Hashaikeh[b,*]

[a] Mechanical Engineering, New York University, Tandon School of Engineering, NY 11201, USA
[b] NYUAD Water Research Center, New York University Abu Dhabi, P.O. Box 129188, Abu Dhabi, UAE

ARTICLE INFO

Method name:
Experimental design approach to TEMD

Keywords:
Design of experiments
Thermal-membrane desalination
Thermoelectricity
Specific energy consumption

ABSTRACT

Thermoelectric membrane distillation has shown promise as a new membrane distillation technique capable of improving energy consumption metrics. This study features an experimental design approach to investigating the performance of a thermoelectric membrane distillation system. Screening and full factorial designs were implemented in Minitab 16 to determine the optimal process conditions for minimizing the specific energy consumption of the system. The process parameter with the most significant impact on the specific energy consumption of thermoelectric membrane distillation systems was determined and a mathematical model for predicting the specific energy consumption was derived. The study showed that adjusting the feed flowrate, the most influential continuous parameter, from a sub-optimal level to an optimal level, while keeping other process variables at their optimal levels, could lead to a 34% reduction in the system's specific energy consumption. At the optimized process parameters of the thermoelectric membrane distillation system, the minimized specific energy consumption fell about 35% below the threshold value of 1,000 kWh/m^3 found among the efficient membrane distillation systems in the literature.

- Thermoelectric heat exchanger provides the driving force for the membrane distillation process
- Seven process variables are assumed to influence the energy consumption of the distillation process
- The variables are screened before being analyzed in a full factorial experimental design

Specifications table

Subject area:	Engineering
More specific subject area:	Thermal-membrane separation
Name of your method:	Experimental design approach to TEMD
Name and reference of original method:	N.A.
Resource availability:	Thermoelectric heat exchanger; Peltier coolers, PTFE membranes; Minitab 16 software

* Corresponding author.
E-mail address: raed.hashaikeh@nyu.edu (R. Hashaikeh).

https://doi.org/10.1016/j.mex.2024.102604
Received 21 November 2023; Accepted 5 February 2024
Available online 6 February 2024

Introduction

Freshwater scarcity is a global problem that is currently being addressed by saline water desalination. Reverse osmosis (RO), multi-stage flash (MSF) and multi-effect distillation (MED) are the most widely adopted desalination technologies [1]. Despite the popularity of these technologies, they have been found unsuitable for small-scale desalination especially in rural or remote areas where access to high-quality energy is limited as well as areas prone to natural disasters [2,3]. This is because MSF and MED have high energy and equipment costs and have associated operational and environmental issues due to the use of fossil fuels [4], while RO is reliant on high-quality electricity in addition to having operational issues like fouling and membrane deterioration [5].

Emerging desalination technologies like membrane distillation (MD) have been proposed as an alternative to the well-established systems [6,7]. In the context of desalination, MD is a thermal process that uses a microporous hydrophobic membrane to distill water from salt solutions. The hydrophobic nature of the membrane keeps the membrane pores dry and retains the salt solution through surface tension, allowing water vapor to diffuse across the membrane [8]. Vapor transport in MD is driven by a vapor pressure gradient maintained across the membrane. To establish this vapor pressure gradient, the saline solution in contact with one side of the membrane is heated while the other side of the membrane is cooled. Although there are several MD configurations in the literature, direct contact membrane distillation, in which the membrane is in direct contact with a liquid phase on either side, is the oldest and most studied MD configuration [9,10]. The commercial deployment of MD as an alternative to RO, MSF and MED for desalination has been largely precluded by the high specific energy consumption (SEC) of MD systems. According to the literature, the SEC of many existing water distillation systems (including MD) ranges from 1,210 – 6,720 kWh/m^3 even with solar heating assistance [4,11]. For MD, many studies have reported a reduction in SEC to a somewhat threshold value of around 1,000 kWh/m^3 through the use of energy recovery devices (ERD) and other techniques [11–16].

Very recently, thermoelectric membrane distillation (TEMD) was proposed as a promising technique for improving the SEC metric for MD systems. In TEMD, a thermoelectric cooler (TEC) is embedded in an MD module to serve two purposes: first, a thermal driver for the process and, second, an ERD to effectively minimize heat exchanger losses to almost zero. This technique is attractive not only because of its ability to minimize energy consumption, but also because of its ability to reduce the equivalent system mass, system complexity, and the required real estate. Lee et al. [17,18] embedded a TEC directly at the membrane surface to treat waste streams generated during space missions. Calculations based on the data reported in their papers, obtained from a series of batch experiments in somewhat air gap MD configuration with no fluid flow, indicated that the SEC was improved to about 2,239 kWh/m^3. Besides the authors' works [19,20], this is the only report of TEMD systems that the authors have found in the literature. Recent works by the authors [19,20] have demonstrated that using TEC as a direct thermal source inside a direct contact membrane distillation (DCMD) module with continuous flow can reduce the SEC by more than 35% below the current threshold and simplify the MD system by eliminating the systems needed for heating, cooling, and recuperative heat recovery. Although these results are promising, the one-variable-at-a-time approach to experimental investigation adopted in these studies makes it challenging to delineate which operational variable has the greatest influence on energy consumption and the conditions that minimize the energy consumption in TEMD.

In the present study, an experimental design approach is taken to understand how the operational variables affect the performance of TEMD systems. For the first time, the variable that has the most significant influence on energy consumption and the optimal conditions that minimize the energy consumption in TEMD systems are determined. The potential interactions between these variables and their effect on system performance are also identified and analyzed. The results of this study are expected to serve as the basis for establishing the specifications needed for advancing TEMD systems to a higher technology readiness level that allows the technology to be more energetically competitive with the likes of RO, MSF and MED for both small- and large-scale desalination.

Method details

Experimental setup

Fig. 1 is a schematic of the TEMD setup used for all the experimental runs. The setup consists of a direct contact membrane distillation (DCMD) module purchased from convergence systems, with an active membrane area of 60 cm^2 and a thermoelectric heat exchanger (TEHX) as the thermal source to drive the distillation process. The TEHX, assembled by sandwiching thermoelectric coolers (TECs) between two water blocks that are made from acrylic, with finned aluminum plates as the heat transfer medium (see Fig. 2), was situated outside the membrane module for convenient operation and precise control of process variables. The electrical leads of the TECs were connected in parallel to a power supply so that the actual current passing through each TEC is the total current divided by the number of TECs installed in the TEHX. For example, each of the 4 TECs installed in the small TEHX will have a current of 1 A and 2.5 A passing through it when a total of 4 A and 10 A are supplied respectively by the power supply unit. The properties of the membranes and TECs used in the experimental setup are provided in Table 1 and Table 2, respectively. Tap water (conductivity ~ 360 μS/cm) was used as the feed while deionized water (conductivity ~ 0.7 μS/cm) was used as the permeate. The choice of tap water feed was to prevent rapid corrosion of the aluminum heat transfer plates in the TEHX, whilst still being able to check for potential wetting of the membrane. Both the feed and permeate streams flowed in countercurrent mode through the TEHX and the DCMD module. The flow conditions are varied according to the screening and factorial designs described in the next sections. Temperatures at the inlet and outlet of the feed and permeate as well as the weight of distillate collected were recorded using a data logger connected to a computer. The distillate flux J (in kg/m^2-h) and the specific energy consumption SEC (in kWh/m^3) were calculated using Eq. (1) and Eq. (2), respectively: where Δm (in kg) is the mass of distillate collected in time Δt (in h), A is

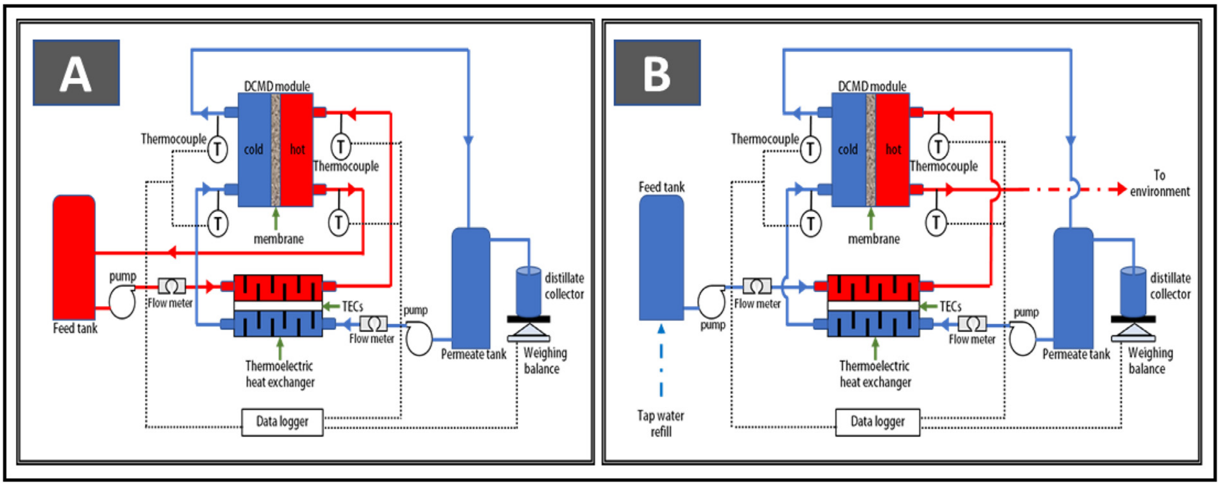

Fig. 1. A schematic of the TEMD setup (a) with hot fluid recirculation and (b) without hot fluid recirculation.

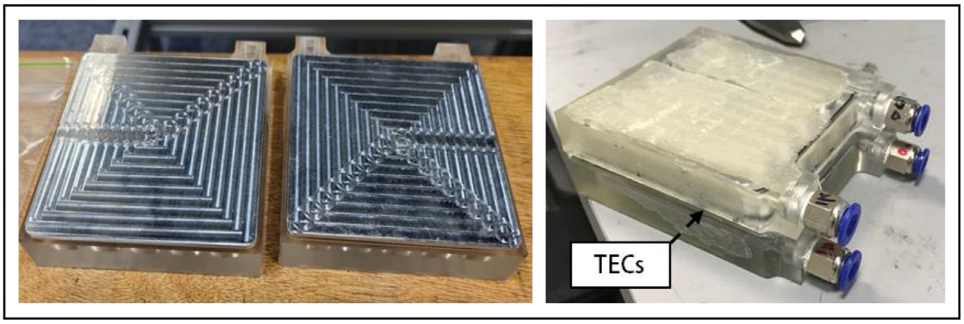

Fig. 2. Water blocks (left) and thermoelectric heat exchanger (right).

Table 1
Characteristics of the MD membranes.

Characteristics	Membrane	
	unlaminated PTFE	Laminated PTFE
Manufacturer	Sterlitech	Sterlitech
Pore size (µm)	0.2	0.2
Liquid Entry Pressure (psi)	40	37
Clean air flow (L/min cm^2) @ 70 mbar	0.34–.94	0.26–0.55
Thickness (µm)	50 (thin)	120 (thick)

Table 2
Characteristics of the thermoelectric coolers.

Characteristics	Thermoelectric coolers	
	TEC1-12706	TEA1-24106
Source	TRU components	Everredtronics
Plate type	Ceramic	Aluminum
Dimensions (L(mm) * W(mm) * H(mm))	40 × 40 × 4.0	40 × 40 × 4.4
Maximum current (A)	6.1	6.0
Maximum cooling power (W)	61.4	67.0
Maximum temperature difference (°C)	70	101
Hot side temperature (°C)	27	30

Table 3
Selected process variables and their levels.

No	Factors	Code	Levels	
			low	High
1	Current (A)	A	4	10
2	Feed flow rate (mL/min)	B	200	800
3	Permeate flow rate (mL/min)	D	200	800
4	Membrane thickness	E	thin	thick
5	Hot fluid recirculation	C	No	Yes
6	TEC plate type	F	ceramic	aluminum
7	TEHX size	G	small	big

Table 4
Screening design table with associated response (SEC) data.

Trial	A	B	D	C	E	F	G	SEC_1	SEC_2
1	4	200	800	no	thick	aluminum	small	3819	3212
2	10	200	200	no	thin	aluminum	big	8289	7958
3	4	800	200	no	thick	ceramic	big	1200	1000
4	10	800	800	no	thin	ceramic	small	3887	4023
5	4	200	800	yes	thin	ceramic	big	609	630
6	10	200	200	yes	thick	ceramic	small	1342	1237
7	4	800	200	yes	thin	aluminum	small	1099	1170
8	10	800	800	yes	thick	aluminum	big	1688	1783

the membrane area (in m^2), P is the electrical power supplied to the TEMD system (in kW) and ρ is the water density (in kg/m^3) [14,15,21].

$$J = \frac{\Delta m}{A \times \Delta t} \tag{1}$$

$$SEC = \frac{P \times \Delta t \times \rho}{\Delta m} \tag{2}$$

In all the experiments, the solutes rejection was calculated from measurements of the final conductivity of the collected distillate and was found to be more than 99% in all cases.

Screening design

To identify the significant main/interaction effects affecting the SEC, a screening design was created in Minitab 16. A total of seven factors (three numeric and four non-numeric) were considered and two levels of each factor were applied. Table 3 lists these factors along with their high and low levels. The levels for the thermoelectric heat exchanger (TEHX) differ by the number of TECs that the aluminum heat transfer plate can accommodate, i.e. small (4 TECs) and big (8 TECs). For the levels of the membrane thickness, refer to Table 1 in the previous subsection. To reduce the number of experimental trials, the 1/16 fraction design with resolution III was used. Therefore, a total of 8 trials with 2 replicates each was obtained. Randomization of the experiments was used to reduce the effect of undesirable disturbances. The experimental layout for the screening of variables and their associated SEC response is shown in Table 4.

Full factorial design

All the factors investigated in the screening step described above were observed to be significant. Given that some of these factors were non-continuous, the best settings for these factors, as given by the response optimizer in Minitab, were chosen and fixed for the full factorial design experiments. Also, since the main effect of the feed flow rate was considerably higher than that of the permeate flow rate, the permeate flow rate was fixed at the best level in the full factorial design. Hence, only the current and feed flow were selected for further analysis. Furthermore, all interaction effects were assumed to be negligible compared to the main effects, which were significant for all the variables.

Each variable in the full factorial design was treated to three levels resulting in $3^2 = 9$ trials with each trial replicated three times to help analyze variability in the SEC as well as reduce errors. The experimental layout for the full 3^2 factorial design is shown in Table 5 with the response (SEC) values recorded at each trial condition.

Method validation

1. Analyzing screening data

Table 5
Full factorial design table with associated response (SEC) data.

Trial	A	B	D	C	E	F	G	SEC_1	SEC_2	SEC_3
1	4	50	800	yes	thick	ceramic	small	1179	1186	1151
2	7	50	800	yes	thick	ceramic	small	1358	1498	1481
3	10	50	800	yes	thick	ceramic	small	1366	1405	1379
4	4	200	800	yes	thick	ceramic	small	979	916	918
5	7	200	800	yes	thick	ceramic	small	1282	1114	1187
6	10	200	800	yes	thick	ceramic	small	1345	1125	1214
7	4	800	800	yes	thick	ceramic	small	625	632	657
8	7	800	800	yes	thick	ceramic	small	930	948	941
9	10	800	800	yes	thick	ceramic	small	1032	929	1098

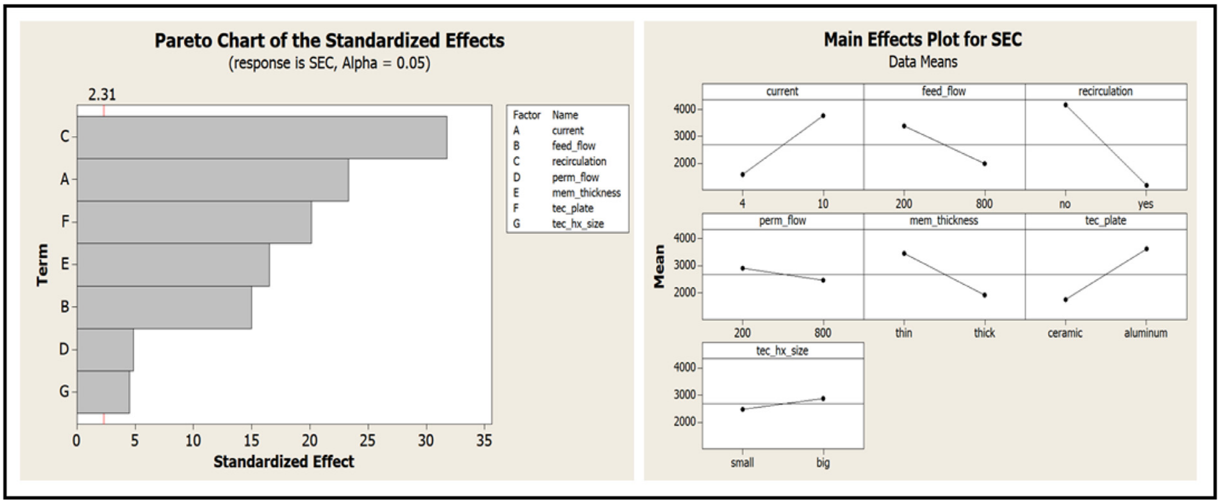

Fig. 3. Pareto chart at 5% significance level (left) and main effects plot for SEC (right).

Analysis of the screening data carried out in Minitab 16 software revealed that all seven process variables considered are significant, with recirculation of the hot fluid having the highest impact on the SEC of the system as shown in the Pareto plot in Fig. 3 (left). The Pareto chart typically plots absolute values of the effects and draws a reference line. Any effect extending beyond this reference line is considered significant. However, because we used replicates, error terms are present and the software displays the absolute values of the standardized effects instead. Since all the effects extend past the reference line at 2.31 standardized value, then all the variables considered are potentially important. However, the degree of their significance is different. A comparison of the relative strengths and direction of effects on the SEC is shown in the main effects plot in Fig. 3 (right). This plot reinforces the information provided in the Pareto chart. The steeper the line in the plot, the greater the effect. Hence, recirculation of the hot fluid has the greatest effect on energy consumption while the size of the thermoelectric heat exchanger has the least effect on energy consumption. It is evident from Fig. 3 (right) that low current, high feed flow rate, hot fluid recirculation, high permeate flow rate, thick membrane, ceramic TECs, and small TEHX are necessary for minimizing the SEC of the system.

In most MD systems, increasing the feed side temperature often leads to a reduction in the SEC because of the increased vapor flux [15,22,23]. Although increasing the current increases the feed side temperature in a TEMD process leading to higher vapor flux, the SEC reduces. This is because the increase electrical work input due to the increasing current outweighs the energy associated with increased vapor production. In the case of feed flowrate, the effect on SEC observed in TEMD systems is consistent with most MD systems. Increasing the feed flow rate increases vapor flux by creating favorable hydrodynamic conditions in the MD module [15]. Increased turbulence and decreased boundary layer resistances are examples of such favorable conditions [24]. Recirculating the hot fluid increases the working temperature on the feed side of the MD module at any value of the electrical work input. This increase in feed side temperature leads to increased vapor flux without any change in the electric work input, and by Eq. (2), results in reduced SEC. Permeate flow rate has the same effect on SEC as the feed flow rate except to a lesser degree due to the lower working temperature at the permeate side of the module. Increasing membrane thickness generally leads to lower flux in MD systems [25] which should increase SEC according to Eq. (2). However, adequately thick membranes minimize conductive heat losses inside a membrane module so that the component of energy transport through the membrane by vapor is greater, leading to lower SEC.

While carrying out the statistical analysis above, it was assumed that the screening data came from a normal distribution. To validate this assumption and the findings from the Pareto chart, a normal probability plot (NPP) of residuals and a histogram of residuals were constructed and the results are displayed in Fig. 4. A residual is the difference between the response value obtained

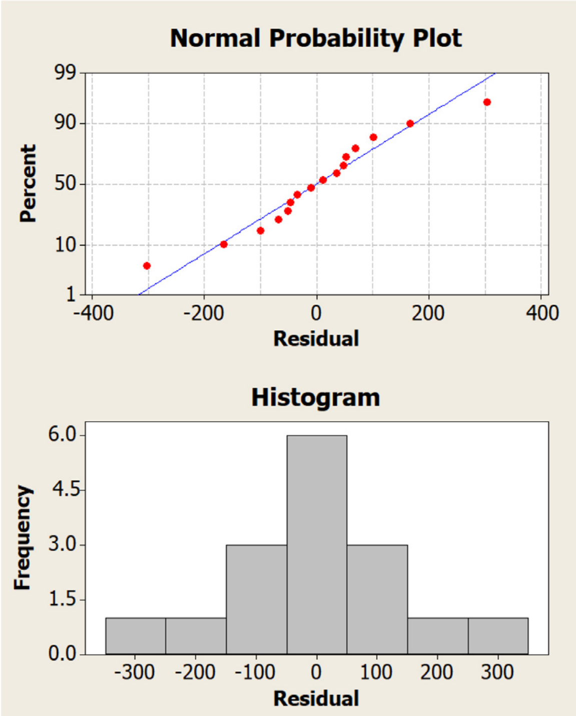

Fig. 4. Normal probability plot and histogram of residuals of the screening data.

Table 6
Analysis of variance table for the factorial design data at a 5% significance level.

Source	Degrees of freedom	Sequential Sum of Squares	Adjusted Sum of Squares	Adjusted Mean Squares	F-value	P-value
A	2	460700	460700	230350	70.19	0.000
B	2	901822	901822	450911	137.39	0.000
AB	4	21887	21887	5472	1.67	0.201
Error	18	59074	59074	3282		
Total	26	1443483				

S = 57.2878 R-Squared = 95.91% R-Squared(adjusted) = 94.09%

from experiment and the predicted response value. Since the residuals lie approximately on a straight line in the normal probability plot and follow a bell-shaped curve of the top of the bars in the histogram, they are normally distributed, and so, our assumption of normally distributed data is valid.

2. Analyzing factorial design data

In the factorial experiments, each of the 9 runs were replicated three times. Just as the screening data was shown to be approximately normally distributed, the full factorial data obtained (Table 5) was also verified to be normally distributed (see Supplementary Information Fig. S1). The analysis of variance (ANOVA) table for the data is shown in Table 6 at a 5% significance level. This 5% significance level (i.e., 95% confidence level) means that any variable with a p-value above 5% is considered insignificant and vice versa. The results in Table 6, therefore, indicates that the main effect of current, A, and feed flow rate, B have a significant impact on the SEC since their p-value is less than 5%. Their interaction effect, AB, however, has no significant influence on SEC since its p-value is above 5%. This conclusion is supported by the interaction plot in Fig. 5 (left) which suggests that there is a weak interaction between the current and the feed flow rate. The weak interaction is signaled by the almost parallel curves of the high and low settings of the current parameter against the feed flow rate parameter. The interpretation of this is that the effect of the current on the SEC is the same irrespective of the setting of the feed flow rate. The same is true for the flow rate which changes the SEC in the same manner regardless of the setting of the current.

While both the current and the feed flow rate are statistically significant, their relative magnitudes and direction of influence are different for the two variables. It is clear from Fig. 5 (right) that the feed flow rate has a stronger influence on the SEC and decreases the SEC as its setting is changed from low to high. This is due to the steeper nature of the SEC versus feed flow curve compared to the SEC versus current curve. The current, which has a weaker influence on the SEC than the feed flow rate, increases the SEC as its setting is changed from low to high. Moreover, the effect of current on SEC from its low setting to its intermediate setting is very

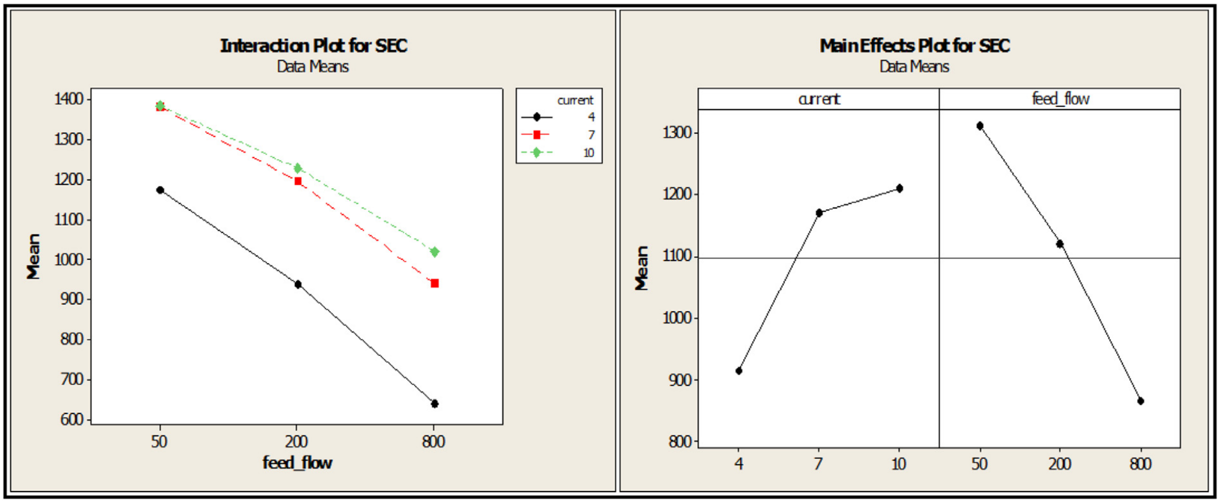

Fig. 5. The interaction (left) and main (rights) plots for SEC means of the factorial data.

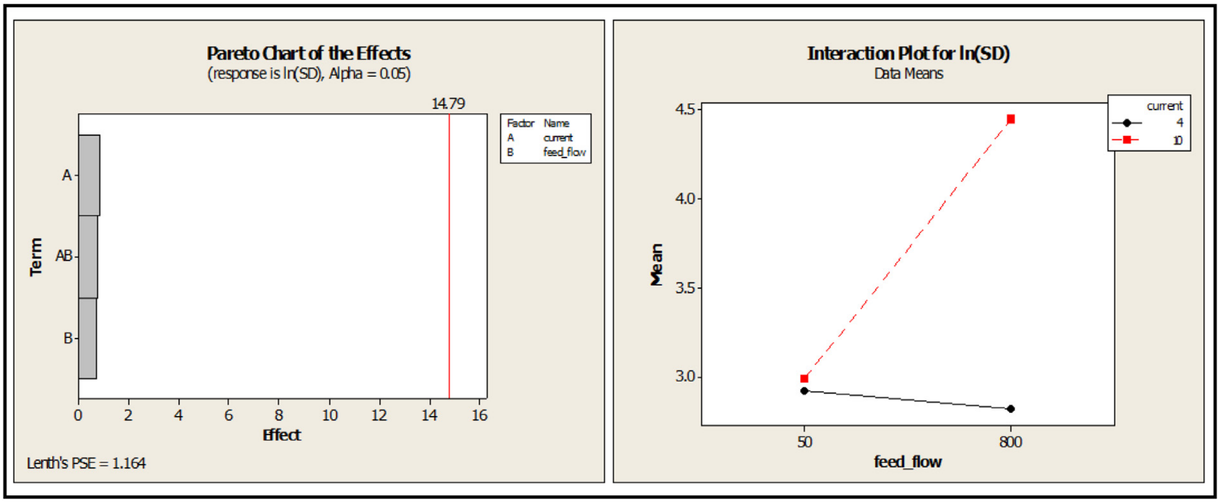

Fig. 6. Pareto plot (left) and interaction plot (right) for SEC variability.

different from its effect from its intermediate setting to its high setting, with the former having a much steeper line than the latter according to Fig. 5 (right). For the feed flow rate, however, its effect on SEC from low setting to intermediate setting is almost the same as that from its intermediate setting to high setting.

3. SEC Minimization

The results of the analyses carried out on the screening and factorial data allowed us to conclude that the SEC of TEMD systems can be minimized by maintaining a high feed flow rate and low current setting, and that SEC is unaffected by the interaction of current and feed flow rate. However, to accept this conclusion, it was important to analyze how the current, feed flow rate, and their interaction affect the variability in SEC. To achieve this, an uncoded design matrix was constructed with only the high and low levels of the factors and the natural logarithm of the standard deviation (SD) in SEC was the response of interest (see Table 7).

Neither the main effect of current and feed flow rate nor their interactions were statistically significant for variability in the SEC of a TEMD system since none of these effects extends to the reference line in the Pareto plot in Fig. 6 (left). Moreover, the interaction plot in Fig. 6 (right) indicates that the variability in SEC is minimized by keeping the current at a low setting and the feed flow rate at a high setting.

Since both the SEC mean and SEC variability are minimized by keeping the current low and the feed flow rate high, the optimal settings for minimizing the SEC of a TEMD system is, thus, to keep the current at a low setting (4 A), wherein 1 A flows through each of the four TECs mounted on the small heat exchanger, keep the feed flowrate at a high setting (800 mL/min), keep the permeate flow rate at high setting (800 mL/min), recirculate the hot fluid back through the heat exchanger, use thick membranes, keep thermoelectric heat exchanger size small (i. e. base plate to accommodate only four TECs), and use TECs with ceramic plates.

Table 7
Uncoded design matrix for SEC variability using the standard deviation (SD).

A	B	D	C	E	F	G	variation in SEC (SD)	ln(SD)
4	50	800	yes	thick	ceramic	small	18.520	2.919
4	800	800	yes	thick	ceramic	small	1358.000	2.823
10	50	800	yes	thick	ceramic	small	1366.000	2.989
10	800	800	yes	thick	ceramic	small	1032.000	4.445

4. Predictive model for the SEC

A model equation for predicting the SEC of a TEMD system was obtained through a regression analysis performed on the data in Table 5. The data was fitted to both linear and nonlinear regression models and the results were compared. It was determined that nonlinear regression was more suitable for fitting the SEC model because statistical analysis of confirmatory tests data showed that the predicted SEC lies within the statistical confidence interval at 99% confidence limit while the predicted SEC from the linear regression model did not. Details of the test data and the calculations can be found in the supplementary information. Eq. (3), derived from a nonlinear regression fitting, gives the SEC as a function of the current A and feed flow rate B, assuming all other factors are kept at their optimal levels.

$$SEC = 1440 - \frac{20743}{A^3} - 0.567B \tag{3}$$

The R-squared value of this linear model was 88.9% (see supplementary information Table S2), indicating that the model is a good fit. According to this equation, a change in the feed flow rate setting from its low level to its high level (optimal setting) at the optimal setting of the current will cause a 34% decrease in the SEC. On the other hand, changing the current setting from high level to low level (its optimal setting) decreases the SEC by 31% at the optimal setting of the feed flow rate. This further affirms the stronger influence that the feed flow rate has on the SEC compared to the current when other process variables are fixed at their optimal setting. Furthermore, when all the process variables are set at their optimal values, the model equation predicts that minimum SEC is achieved with a value of about 662 kWh/m^3. This value is approximately 34% below the threshold found among the best MD systems in the literature.

Conclusions

This paper has presented an experimental investigation to understand how operational variables affect the performance of thermoelectric membrane distillation systems. The variables with significant influence on energy consumption and the setting of these variable that minimizes energy consumption of the system were delineated using experimental design. Additionally, potential interactions between the variables and their effect on system performance were identified and analyzed. From the results, it was concluded that thermoelectric membrane distillation system performance is influenced by all its operational variables, but to different degrees. Contrary to previous reports suggesting that the electric current is the most significant operational variable affecting energy consumption, this work showed that the feed flow rate, in fact, has the most significant impact on the energy consumption when other variables are kept at their optimal levels. According to a nonlinear model developed in this work for predicting the specific energy consumption of the thermoelectric membrane distillation system, adjusting the feed flowrate from its low level to its high level (optimal setting) at the optimal current setting results in a 34% reduction in specific energy consumption, whereas changing the current from its high level to its low level (optimal setting) at the optimal feed flow rate setting leads to a 31% decrease in specific energy consumption. The results obtained in this work further concluded that when all process variables are at their optimal level, specific energy consumption is minimized. Based on the model prediction, the minimized specific energy consumption is about 35% below the 1,000 kWh/m^3 threshold found among the efficient membrane distillation systems in the literature, similar to previous reports on thermoelectric membrane distillation systems. Indeed, the results presented in this study may be used to develop the requirements for a higher technology readiness level thermoelectric membrane distillation system.

Ethics statements

This work did not involve human subjects, animal experiments, or data collected from social media platforms

Declaration of competing interest

The authors declare that they have no known competing financial interests or personal relationships that could have appeared to influence the work reported in this paper.

CRediT authorship contribution statement

Olawale Makanjuola: Conceptualization, Visualization, Methodology, Investigation, Data curation, Writing – original draft, Resources. **Raed Hashaikeh:** Supervision, Funding acquisition, Writing – review & editing.

Data availability

No data was used for the research described in the article.

Acknowledgments

General: The Authors would like to acknowledge the support of the Core Technology Platforms team at New York University Abu Dhabi for their assistance with the fabrication of the thermoelectric heat exchangers.

Funding: This work was supported by the NYUAD Water Research Center and funded by Tamkeen under the NYUAD Research Institute Award with project number CG007.

Supplementary materials

Supplementary material associated with this article can be found, in the online version, at doi:10.1016/j.mex.2024.102604.

References

[1] Y. Tokui, H. Moriguchi, Y. Nishi, Comprehensive environmental assessment of seawater desalination plants: multistage flash distillation and reverse osmosis membrane types in Saudi Arabia, (2014). doi:10.1016/j.desal.2014.07.034.
[2] A. Deshmukh, C. Boo, V. Karanikola, S. Lin, A.P. Straub, T. Tong, D.M. Warsinger, M. Elimelech, Membrane distillation at the water-energy nexus: limits, opportunities, and challenges, Energy Environ. Sci. 11 (2018) 1177–1196, doi:10.1039/c8ee00291f.
[3] H.C. Duong, L.T.T. Tran, H.T. Truong, B. Nelemans, Seawater membrane distillation desalination for potable water provision on remote islands – a case study in Vietnam, Case Stud. Chem. Environ. Eng. 4 (2021) 100110, doi:10.1016/J.CSCEE.2021.100110.
[4] H. Al-Madhhachi, G. Min, Effective use of thermal energy at both hot and cold side of thermoelectric module for developing efficient thermoelectric water distillation system, Energy Convers. Manag. 133 (2017) 14–19, doi:10.1016/J.ENCONMAN.2016.11.055.
[5] K. Ali, A.A. Alwan, S. Bahayan, E. Alhseinat, M.I. Hassan Ali, A numerical analysis of the electromagnetic field effect on direct contact membrane distillation performance, Energy Convers. Manag. 292 (2023) 117328, doi:10.1016/J.ENCONMAN.2023.117328.
[6] D. Winter, Membrane Distillation: A Thermodynamic, Technological and Economic Analysis, Filderstadt Shak. Verlag, 2014.
[7] B.B. Ashoor, S. Mansour, A. Giwa, V. Dufour, S.W. Hasan, Principles and applications of direct contact membrane distillation (DCMD): a comprehensive review, Desalination 398 (2016) 222–246, doi:10.1016/J.DESAL.2016.07.043.
[8] L. Peña, J.M.O. De Zárate, J.I. Mengual, Steady states in membrane distillation: influence of membrane wetting, J. Chem. Soc. Faraday Trans. 89 (1993) 4333–4338, doi:10.1039/FT9938904333.
[9] M.S. Khayet, T. Matsuura, Membrane Distillation: Principles and Applications, Elsevier, 2011 https://www.sciencedirect.com/science/book/9780444531261 (accessed February 27, 2018).
[10] K. Rahaoui, L.C. Ding, L.P. Tan, W. Mediouri, F. Mahmoudi, K. Nakoa, A. Akbarzadeh, Sustainable membrane distillation coupled with solar pond, in: Energy Procedia, Elsevier Ltd, 2017, pp. 414–419, doi:10.1016/j.egypro.2017.03.162.
[11] J. Choi, J. Cho, J. Shin, H. Cha, J. Jung, K.G. Song, Performance and economic analysis of a solar membrane distillation pilot plant under various operating conditions, Energy Convers. Manag. 268 (2022) 115991, doi:10.1016/J.ENCONMAN.2022.115991.
[12] F. Suárez, R. Urtubia, Tackling the water-energy nexus: an assessment of membrane distillation driven by salt-gradient solar ponds, Clean Technol. Environ. Policy 18 (2016) 1697–1712, doi:10.1007/s10098-016-1210-3.
[13] W. Jantaporn, A. Ali, P. Aimar, Specific energy requirement of direct contact membrane distillation, Chem. Eng. Res. Des. 128 (2017) 15–26, doi:10.1016/j.cherd.2017.09.031.
[14] F.E. Ahmed, B.S. Lalia, R. Hashaikeh, N. Hilal, Enhanced performance of direct contact membrane distillation via selected electrothermal heating of membrane surface, J. Memb. Sci. 610 (2020) 118224, doi:10.1016/j.memsci.2020.118224.
[15] M.R. Elmarghany, A.H. El-Shazly, M.S. Salem, M.N. Sabry, N. Nady, Thermal analysis evaluation of direct contact membrane distillation system, Case Stud. Therm. Eng. 13 (2019) 100377, doi:10.1016/J.CSITE.2018.100377.
[16] K. Okiel, A.H.M. El-Aassar, T. Temraz, S. El-Etriby, H.A. Shawky, Vacuum enhanced direct contact membrane distillation for oil field produced water desalination: specific energy consumption and energy efficiency, Desalin. Water Treat. 57 (2016) 11945–11955, doi:10.1080/19443994.2015.1048305.
[17] J.M. Lee, L. Delzeit, J. Parodi, G. Pace, S. Trieu, Membrane distillation driven by embedded thermoelectric heat pump, in: Proceedings of the 48th International Conference on Environmental Systems, 2018.
[18] J. Parodi, J. Lee, S. Trieu, G. Pace, Thermoelectric membrane distillation system engineering design improvement concepts, in: Proceedings of the 49th International Conference on Environmental Systems, 2019.
[19] O. Makanjuola, B.S. Lalia, R. Hashaikeh, Thermoelectric heating and cooling for efficient membrane distillation, Case Stud. Therm. Eng. 28 (2021) 101540, doi:10.1016/J.CSITE.2021.101540.
[20] O. Makanjuola, R. Hashaikeh, Numerical and experimental investigation of thermoelectric materials in direct contact membrane distillation, Energy Convers. Manag. 267 (2022) 115880, doi:10.1016/j.enconman.2022.115880.
[21] M. Mustakeem, A. Qamar, A. Alpatova, N. Ghaffour, Dead-end membrane distillation with localized interfacial heating for sustainable and energy-efficient desalination, Water Res. 189 (2021) 116584, doi:10.1016/J.WATRES.2020.116584.
[22] F. Han, S. Liu, K. Wang, X. Zhang, Enhanced performance of membrane distillation using surface heating process, Membranes (Basel) 11 (2021), doi:10.3390/MEMBRANES11110866.
[23] A. Najib, J. Orfi, H. Alansary, E. Ali, Assessing the impact of operating conditions on the energy and exergy efficiency for multi-effect vacuum membrane distillation systems, Water 13 (2021) 1500 2021VolPage131500, doi:10.3390/W13111500.
[24] I. Janajreh, K. El Kadi, R. Hashaikeh, R. Ahmed, Numerical investigation of air gap membrane distillation (AGMD): seeking optimal performance, Desalination 424 (2017) 122–130, doi:10.1016/J.DESAL.2017.10.001.
[25] L. Martínez, J.M. Rodríguez-Maroto, Membrane thickness reduction effects on direct contact membrane distillation performance, J. Memb. Sci. 312 (2008) 143–156, doi:10.1016/j.memsci.2007.12.048.